COMPOSITE GRID METHOD FOR HYBRID SYSTEMS

J. Fish, V. Belsky and M. Pandheeradi
Department of Civil Engineering and Scientific Computation
Research Center,
Rensselaer Polytechnic Institute, Troy, NY 12180, USA

Abstract

A Composite grid method is developed for solving symmetric indefinite linear systems arising from the three-field hybrid variational principle, which weakly enforces compatibility and traction continuity conditions between independently modeled substructures. The positive definite global problem and the indefinite local system are derived using minimization on the subspace and the stationarity principle, respectively. The indefinite local problem is then transformed into an equivalent symmetric positive definite system, which can be subsequently solved by either a direct solver without pivoting or a preconditioned iterative method. Alternative semi-iterative solution procedures for the case when auxiliary coarse grid is not available, are also described. Numerical performance studies for two-dimensional plane stress and shell problems are carried out to test the usefulness of the proposed procedures.

1 Introduction

The term *global-local finite element analysis* was originally coined by Mote [1], in the context of enriching finite element (local) interpolants with special (global) shape functions known to approximately represent the exact solution. Since then, global-local techniques have undergone many interesting twists, not even remotely resembling their predecessor, although

their primary goal of reliably predicting the global response and capturing local effects of interest at minimum computational cost remains the same.

Since the pioneering work of Mote in 1971, the literature on what has been or could have been interpreted as global-local analysis/modeling techniques, has grown at an astonishing rate. We refer to [2] for extensive review on global-local strategies and to [3], [4] on various aspects of reliability including adaptivity, convergence and accuracy of global-local techniques. Here, we focus only on the class of global-local techniques which advocates hierarchical solution strategy in the sense that the information from the global analysis is exploited in resolving local effects.

Among the most popular hierarchical global-local strategies are various forms of multigrid and composite-grid methods ([5]-[10]) as well as methods based on hierarchical decomposition of approximation space ([11]-[15]). Engineering global-local approaches, which approximate a detailed response by means of postprocessing techniques, such as subjecting a locally refined model to the boundary conditions extracted from the global grid, can be viewed as a single iteration within the composite grid procedure. For various improvements of this simple 'zoom' technique we refer to ([16]-[18]).

Recent numerical studies conducted at NASA Langley [19] have revealed that among various global-local interface formulations for independently modeled substructures with nonmatching nodes, an optimal solution accuracy in the vicinity of the interface is obtained by weakly enforcing compatibility and traction continuity conditions. A simple patch test, consisting of two independently modeled substructures subjected to a constant strain field as shown in Figure 1, has been devised in [20] to test the quality of the interface modeling. The distribution of σ_{xx} in Figure 1 reveals that if substructure interface nodes (considered as slave nodes) are constrained to deform in the pattern prescribed by the independently discretized interface (the nodes of which are considered as master nodes) with either piecewise linear or spline interpolation functions, the error in the stress field could be as high as 110% compared to the exact solution. On the other hand, by weakly enforcing compatibility and traction continuity conditions at the interface, the aforementioned patch test is exactly satisfied for both discretizations of the interface and piecewise constant approximation of Lagrange multipliers.

Semi-iterative procedures for solving domain decomposition problems arising from the two- and three- field hybrid variational principles have been reported in [21],[22] and [20],

respectively. Sufficient solvability conditions for hybrid domain decomposition methods have been established in [23] in the context of *mortar* spaces. The primary objective of the present manuscript is to generalize hierarchical global-local procedures in the spirit of composite grid (FAC [5]) and adaptive multigrid (MLAT [10]) methods for indefinite linear systems arising from the three-field hybrid variational formulation, which enforces compatibility between independently modeled substructures in the weak sense.

The contents of the paper are as follows. In Section 2 we derive the positive definite global problem and the indefinite local system using minimization on the subspace and the stationarity principle, respectively. In Section 3 the indefinite local problem is transformed into an equivalent symmetric positive definite system, which is then solved by either a direct solver without pivoting or a preconditioned iterative method. Section 4 describes alternative semi-iterative solution procedures for the case when an auxiliary coarse grid is not available. Numerical performance studies and comparisons conclude the manuscript.

2 Formulation

Let Ω denote the domain of the problem, that has an initial finite element discretization G. Now assume that based on the information provided by the aposteriori discretization error indicators, a subdomain $\Omega^L \subset \Omega$ is refined by introducing smaller elements in order to achieve a better resolution of solution in that region. The new model consists of the finite element grid G^G on $\Omega^G = \Omega \setminus \Omega^L$, where the discretization coincides with G; G^L, the local or refined grid on the region Ω^L; and G_s, the independent discretization of the interface between the two grids. The initial grid G will serve as the auxiliary grid G^A in the composite grid solution of the three-field hybrid variational formulation.

In order to facilitate the formulation of the problem, we introduce the following notations, as shown in Figure 2. Subscript "$_B$" will be used to identify the part of a particular grid at the boundary at the interface, and subscripts "$_G$" and "$_L$" will refer to the rest of the grid depending on whether it is in the region of Ω^G or Ω^L. The superscripts "^{G}", "^{L}" and "^{A}" as introduced earlier will determine the source grid or discretization. Accordingly, note that $G^A = G^A_G \cup G^A_B \cup G^A_L$, where $G^A_G = G^G_G$, $G^A_B = G^G_B$ and G^A_L is the initial discretization on Ω^L. The same convention will be adopted to refer to the vectors associated with each grid. For example, d^G and d^L are the the displacement vectors on grids G^G and G^L and can be

partitioned as follows:

$$d^G = \begin{bmatrix} d^G_G \\ d^G_B \end{bmatrix}; \qquad d^L = \begin{bmatrix} d^L_L \\ d^L_B \end{bmatrix} \tag{1}$$

The auxiliary grid displacements d^A will have the partition $d^A = [d^A_G \quad d^A_B \quad d^A_L]^T$. Note that $d^A_G = d^G_G$ and $d^A_B = d^G_B$.

The solution quantities associated with the interface grid G_s will be characterized by the subscript s. For example, the displacement vector corresponding to the interface discretization G_s is denoted by d_s.

Following the above notations, we introduce the three-field hybrid functional

$$\begin{aligned} \Psi \;=\; & \frac{1}{2}[(K^G d^G, d^G) + (K^L d^L, d^L)] - (F^G, d^G) - (F^L, d^L) \\ & + \int_S \lambda^G (u_s - u^G_B)\, dS + \int_S \lambda^L (u_s - u^L_B)\, dS \Rightarrow \text{stationary} \end{aligned} \tag{2}$$

where K^G and K^L represent the stiffness matrices of grids G^G and G^L respectively, λ^G and λ^L the fields of Lagrange multipliers for weakly enforcing compatibility conditions along the boundaries G^G_B and G^L_B respectively, u_s is the interface displacement field, and u^G_B and u^L_B are the displacements of grids G^G_B and G^L_B. F^G and F^L are the external load vectors associated with grids G^G and G^L respectively. Even though the three-field hybrid variational principle and the proposed hybrid composite grid method can be readily extended to the general case of multiple local domains and multiple interfaces, we limit our presentation to problems with single local domain for the sake of clarity.

Next, we define the prolongation operators that transfer solution information between the auxiliary grid and the grids corresponding to the composite model. Specifically, T^G is the prolongation operator from G^A to G^G, while T^L and T_s communicate between G^A and G^L, and G^A and G_s respectively, i.e.:

$$T^G : G^A \rightarrow G^G \tag{3}$$

$$T^L : G^A \rightarrow G^L \tag{4}$$

$$T_s : G^A \rightarrow G_s \tag{5}$$

In the above, T^G is simply an orthogonal assembly operator consisting of identity matrix corresponding to the part of G^A coinciding with G^G, namely $G^A_G \cup G^A_B$, and zero corresponding

to the remaining part of G^A, as shown below:

$$T^G = \begin{bmatrix} I & 0 & 0 \\ 0 & I & 0 \end{bmatrix} \tag{6}$$

T^L is formed from the auxiliary grid shape functions N^A evaluated at the nodal points of the local grid G^L. Symbolically,

$$T^L = \begin{bmatrix} 0 & 0 & N^A(X_L^L) \\ 0 & N^A(X_B^L) & 0 \end{bmatrix} \tag{7}$$

where X_B^L and X_L^L are the coordinates of local grid nodes at the interface and interior respectively.
Similarly, T_s is formed from the auxiliary grid shape functions at the boundary at the interface, evaluated at the interface grid points.

$$T_s = [0 \quad N^A(X_s) \quad 0] \tag{8}$$

where X_s are the coordinates of the interface grid nodes.

As a prelude to the statement of the discretized version of the problem defined on the new model (2), we define the generalized displacement interpolations for the grids G^G, G^L and G_s as well as the interpolation for Lagrange multipliers. We start with the generalized displacement interpolation for the interface

$$u_s = N_s d_s \tag{9}$$

where N_s is the matrix of interpolating functions and d_s is the generalized displacement vector associated with the interface nodes. Let N_B^G and N_B^L denote the interpolation functions for the boundary displacements of grids G^G and G^L respectively at the interface, which follow from the finite element discretization on the corresponding grids. Finally, the Lagrange multipliers λ^G and λ^L for grids G^G and G^L at the interface are interpolated from the respective discrete values Λ^G and Λ^L associated with the finite element edges (for 2-dimensional

or shell problems) of the two grids at the interface

$$\lambda^G = R^G \Lambda^G \tag{10}$$

$$\lambda^L = R^L \Lambda^L \tag{11}$$

Substitution of these discretizations in the three-field hybrid variational form yields the following statement of the discretized version of the problem:
Find generalized displacements (d^G, d^L, d_s) and Lagrange multipliers (Λ^G, Λ^L) such that

$$\Psi(d^G, d^L, d_s, \Lambda^G, \Lambda^L) = \Pi + (\Lambda^G, \phi^G) + (\Lambda^L, \phi^L) \Rightarrow (d^G, \overset{\min}{d^L}, d_s), \quad (\overset{\max}{\Lambda^G}, \Lambda^L) \tag{12}$$

where

$$\Pi = \frac{1}{2}[(K^G d^G, d^G) + (K^L d^L, d^L)] - (F^G, d^G) - (F^L, d^L) \tag{13}$$

and the vectors ϕ^G and ϕ^L are defined by:

$$\phi^G \equiv J^{GT} d_s + M^{GT} d^G \tag{14}$$

and

$$\phi^L \equiv J^{LT} d_s + M^{LT} d^L \tag{15}$$

Matrices M^G and M^L have the forms:

$$M^{GT} = [0 \quad M_B^{GT}], \quad M^{LT} = [0 \quad M_B^{LT}] \tag{16}$$

J^G and M_B^G as well as J^L and M_B^L are integrated quantities over the interface, given by:

$$J^G = \int_S N_s^T R^G \, dS, \qquad M_B^G = -\int_S N_B^{GT} R^G \, dS \tag{17}$$

and

$$J^L = \int_S N_s^T R^L \, dS, \qquad M_B^L = -\int_S N_B^{LT} R^L \, dS \tag{18}$$

Equation (12) can be equivalently stated as a constrained optimization problem:

$$\Pi \Rightarrow (d^G, \overset{\min}{d^L}, d_s) \tag{19}$$

subject to the constraints

$$\phi^G(d^G, d_s) = 0; \quad \phi^L(d^L, d_s) = 0 \tag{20}$$

We propose to solve the system (12) based on the Composite Grid philosophy, using the initial grid G as the auxiliary grid G^A to capture the lower frequency response of the new model within a two-level iterative scheme. We refer to the problem on grid G^A as the "global" problem. The oscillatory or the localized part of the response is resolved on grids G^L and G_s by transforming the corresponding indefinite system into an equivalent positive definite system which is then solved either exactly using a direct solver without pivoting or approximately using a preconditioned iterative solver. We refer to the problem on G^L and G_s as the "local" problem. During the solution of the local problem, displacements d^G on G^G are held fixed.

2.1 Formulation of the global problem

Find the correction v^A that minimizes Ψ on the subspace of the auxiliary grid functions:

$$\Psi({}^i d^G + T^G v^A, {}^i d^L + T^L v^A, {}^i d_s + T_s v^A, {}^i\Lambda^G, {}^i\Lambda^L) \Rightarrow \overset{\min}{(v^A)} \tag{21}$$

which yields

$$(T^{G^T} K^G T^G + T^{L^T} K^L T^L) v^A = T^{G^T}({}^i r^G - M^G\, {}^i\Lambda^G) + T^{L^T}({}^i r^L - M^L\, {}^i\Lambda^L) - T_s^T(J^G\, {}^i\Lambda^G + J^L\, {}^i\Lambda^L) \tag{22}$$

where ${}^i r^G = F^G - K^G\, {}^i d^G$ and ${}^i r^L = F^L - K^L\, {}^i d^L$ are the residuals in the grids G^G and G^L respectively. Left superscript $({}^i)$ refers to the global-local cycle count. In (22) we introduce the approximation $K^A \approx T^{G^T} K^G T^G + T^{L^T} K^L T^L$ where K^A is the auxiliary grid stiffness matrix. This will reduce the computational effort significantly, since K^A is already available in the factorized form, being the stiffness matrix corresponding to the initial discretization G. It will be shown later that, provided the local problem is solved exactly, the two parts on the right hand side in (22), namely ${}^i r^L - M^L\, {}^i\Lambda^L$ and $J^G\, {}^i\Lambda^G + J^L\, {}^i\Lambda^L$ would each vanish

and we will be left with the following as the auxiliary or global system:

$$K^A v^A = T^{GT}({}^i r^G - M^G \, {}^i\Lambda^G) \tag{23}$$

Solution v^A of (23) (or (22)) is prolongated back to grid G^G to obtain the corrected displacements ${}^i d^G \leftarrow {}^i d^G + T^G v^A$. We would like to point out that the solution, after the auxiliary grid correction, doesn't necessarily satisfy the constraints ${}^i\phi^G = 0$. In other words, $J^{GT} \, {}^i d_s + M^{GT} \, {}^i d^G \neq 0$ in general. This violation of constraints following auxiliary grid correction is rectified during the solution of the local problem so that at the end of each two-level cycle the solution satisfies the constraints ${}^i\phi^G = 0$ and ${}^i\phi^L = 0$.

2.2 Formulation of the local problem

Find the displacement correction $v = [v^L \quad v_s]^T$ and Lagrange multipliers (Λ^G, Λ^L) such that

$$\Psi({}^i d^G, {}^i d^L + v^L, {}^i d_s + v_s, \Lambda^G, \Lambda^L) \Rightarrow \overset{\min}{(v^L, v_s)} \quad \overset{\max}{(\Lambda^G, \Lambda^L)} \tag{24}$$

which yields the system of equations:

$$Kv = {}^i r - Q\Lambda \tag{25}$$

$$Q^T v = {}^i\phi \tag{26}$$

where $Q^T = [0 \quad M^T \quad J^T]$ with $M^T = \begin{bmatrix} 0 \\ M_B^{LT} \end{bmatrix}$ and $J^T = \begin{bmatrix} J^{GT} \\ J^{LT} \end{bmatrix}$, $\Lambda = [\Lambda^G \quad \Lambda^L]^T$, ${}^i\phi = [-{}^i\phi^G \quad -{}^i\phi^L]^T$, ${}^i r = [{}^i r^L \quad {}^i r_s]^T$ with ${}^i r^L = F^L - K^L \, {}^i d^L$ and ${}^i r_s = 0$, K is a block diagonal semidefinite stiffness matrix with K^L as the block corresponding to grid G^L and zero block corresponding to the interface grid G_s. K^L has the partitioning

$$K^L = \begin{bmatrix} K^L_{LL} & K^L_{LB} \\ K^L_{BL} & K^L_{BB} \end{bmatrix} \tag{27}$$

Equivalently, the local problem can be stated as:

$$\frac{1}{2}(Kv, v) - ({}^i r, v) \Rightarrow \min \tag{28}$$

subject to the constraints:

$$Q^T v = {}^i\phi \tag{29}$$

Similar to the use of K without any right superscript or subscript, vectors of nodal quantities corresponding to the grid $G_s \cup G^L$ are denoted without any right indices, like ${}^i r$ for residual and ${}^i d$ for displacements at the end of cycle i.

It should be noted that no nodal correspondence is assumed between G^G and G^L at the interface. Furthermore, the coupling between G^G and G^L is only through the special interface degrees of freedom on G_s by means of independent sets of Lagrange multipliers.

3 The Solution of the Local Problem

The linear system of equations resulting from the local problem is once again reproduced below:

$$Kv = {}^i r - Q\Lambda \tag{30}$$

$$Q^T v = {}^i\phi \tag{31}$$

It is easy to see that the exact solution of (30) and (31) implies:

$${}^{i+1}r - Q\Lambda = 0 \tag{32}$$

where ${}^{i+1}r = {}^i r - Kv$. On substitution of appropriate quantities, (32) simplifies to: ${}^{i+1}r^L - M^L\Lambda^L = 0$ and $J^G\Lambda^G + J^L\Lambda^L = 0$, giving rise to equation (23) as discussed earlier. We proceed to obtain the solution of the system (30) and (31) in two stages. In the first stage, Δv is computed as minimum correction that satisfies the non-homogeneous part of the constraint equations (31) which is introduced due to the auxiliary grid correction. The problem for the minimum correction Δv is formulated as follows:

$$\frac{1}{2}(\Delta v, \Delta v) \Rightarrow \min \tag{33}$$

subject to

$$Q^T\, \Delta v = {}^i\phi \tag{34}$$

It is easily verified that Δv is obtained as:

$$\Delta v = Q(Q^T Q)^{-1}\, {}^i\phi \tag{35}$$

After the first stage solution, the displacements ${}^i d$ and residual ${}^i r$ may be updated according to:

$${}^i d \longleftarrow {}^i d + \Delta v \tag{36}$$

$${}^i r \longleftarrow {}^i r - K\, \Delta v \tag{37}$$

The displacements ${}^i d^G$ and ${}^i d$ now satisfy the constraints ${}^i \phi^G = 0$ and ${}^i \phi^L = 0$.

In the second stage, one has to solve the system

$$Kv = {}^i r - Q\Lambda \tag{38}$$

with homogeneous constraints

$$Q^T v = 0 \tag{39}$$

For simplicity of presentation, we reformulate (38) and (39) in terms of the total displacement vector d, which is the sum of the displacements after the first stage solution ${}^i d$ and the correction to be solved for in the second stage, namely v. In other words,

$$d = {}^i d + v \tag{40}$$

Thus the equivalent system of equations becomes:

$$Kd = F - Q\Lambda \tag{41}$$

$$Q^T d = 0 \tag{42}$$

It should be mentioned that if the solution of (41, 42) is carried out by some iterative procedure, it will be mandatory that the initial guess for the solution be ${}^i d$.
We refer to (41, 42) as the source problem defined on the local and interface grids, $G_s \cup G^L$.

Since the generalized stiffness matrix K is semidefinite, one can adopt a classical, projected conjugate gradient method for the solution of the source problem, ensuring that the

constraints are satisfied at every iteration [24]. As a prelude to our subsequent derivation, we describe this procedure in some detail, emphasizing the "projection" approach as a method of enforcing the constraints. The projection operator P generates projected generalized displacement vector d', defined as $d' = Pd$, that satisfies the constraint equation $Q^T d' = 0$. Projected vector d' is the closest vector to d in the Euclidian norm that satisfies the constraint equation $Q^T d' = 0$. Mathematically, the problem of finding the projection operator P can be stated as follows:
Given Q and d. Find d' and Λ such that $\frac{1}{2}(d - d', d - d') + (\Lambda, Q^T d')$ is stationary. The resulting linear system is given by:

$$d' - d + Q\Lambda = 0 \tag{43}$$

$$Q^T d' = 0 \tag{44}$$

from which one obtains,

$$d' = Pd, \qquad P = I - Q(Q^T Q)^{-1} Q^T \tag{45}$$

Substituting for Q yields,

$$P = \begin{bmatrix} I & 0 & 0 \\ 0 & I - Mq^{-1}M^T & -Mq^{-1}J^T \\ 0 & -Jq^{-1}M^T & I - Jq^{-1}J^T \end{bmatrix} \equiv \begin{bmatrix} I & 0 & 0 \\ 0 & P_{BB} & P_{Bs} \\ 0 & P_{sB} & P_{ss} \end{bmatrix} \tag{46}$$

where $q \equiv Q^T Q = M^T M + J^T J$.
Provided the source problem has a unique solution $[d \quad \Lambda]^T$, it can be easily verified that the projection operator P and the constraint matrix Q satisfy the following properties:
(i) $Q^T Q$ is nonsingular
(ii) $Q^T P = PQ = 0$
(iii) $Q^T d = 0 \Leftrightarrow Pd = d$

The classical, projected conjugate gradient algorithm for the solution of the source (local) problem is summarized below:

$${}_0d = {}^i d, \quad {}_0r' = F - K\ {}_0d, \quad {}_0r = P\ {}_0r', \quad {}_0v = {}_0r \tag{47}$$

Do for $j = 1, 2...$until convergence

$$
\begin{aligned}
{}_j\gamma &= ({}_{j-1}r, {}_{j-1}v)/(K\ {}_{j-1}v, {}_{j-1}v) && (48)\\
{}_jd &= {}_{j-1}d + {}_j\gamma\ {}_{j-1}v && (49)\\
{}_jr' &= {}_{j-1}r - {}_j\gamma K\ {}_{j-1}v && (50)\\
{}_jr &= P\ {}_jr' && (51)\\
{}_j\beta &= ({}_jr, {}_jr)/({}_{j-1}r, {}_{j-1}r) && (52)\\
{}_jv &= {}_jr + {}_j\beta\ {}_{j-1}v && (53)
\end{aligned}
$$

In the absence of a natural preconditioner to accelerate the rate of convergence, the classical projected conjugate gradient algorithm is of little practical use in solving the local problem. This is especially so in the case of shells, where the problem is inherently ill-conditioned. In the next section, we transform the non-positive definite local problem into an equivalent positive definite system, that can be solved either directly without pivoting, or by the application of some iterative solution scheme such as conjugate gradient method with suitable preconditioners.

3.1 The Formulation of an Equivalent Positive Definite System

The transformation of the linear system (41, 42) into an equivalent positive definite system is essentially based on two assertions stated below with proofs:

Assertion 1: The system (41, 42) is equivalent to the system:

$$PKPd = PF \tag{54}$$

$$d = Pd \tag{55}$$

provided the source (local) problem has a unique solution for any right hand side vector.

Proof: From the properties of the projection operator P and constraint matrix Q presented earlier, it immediately follows that if $Kd + Q\Lambda = F$ and $Q^Td = 0$, the relations $PKPd = PF$ and $d = Pd$ will hold.

It remains to be shown that the vice-versa is also true. Let d be a solution of the system

$PKPd = PF$. Denote $\tilde{d} = Pd$.

We have $\tilde{d} = P\tilde{d} \Rightarrow Q^T\tilde{d} = 0$. Also,

$PKP\tilde{d} = PF$ or, $PK\tilde{d} = PF \Rightarrow K\tilde{d} = F + Z$

where Z belongs to the subspace of vectors that satisfy $PZ = 0$, i.e, belongs to the Kernel of P.

Now, $PZ = 0 \Rightarrow Z = Q\overbrace{(Q^TQ)^{-1}Q^TZ}^{-\Lambda} \equiv -Q\Lambda$

In other words, $K\tilde{d} + Q\Lambda = F$ and $Q^T\tilde{d} = 0$. This concludes the proof.

Assertion 2 If the source problem has a unique solution, there exists an equivalent positive definite system:

$$\bar{K}d = PF \tag{56}$$

where $\bar{K}$ is a positive definite matrix defined by

$$\bar{K} = PKP + \alpha QQ^T, \qquad \alpha > 0 \tag{57}$$

Moreover, the solution of the positive definite system will be independent of α.

Proof: We first prove the positive definiteness of $\bar{K}$. Let x be an arbitrary nonzero vector.

$(\bar{K}x, x) = (KPx, Px) + \alpha(Q^Tx, Q^Tx)$

Consider the two possibilities:

(i) $Q^Tx \neq 0 \quad \forall x \Rightarrow (\bar{K}x, x) > 0$ since K is semidefinite.

(ii) $Q^Tx = 0 \Rightarrow Px = x$. In this case we exploit the uniqueness of the solution of the source problem to conclude that $(\bar{K}x, x) = (Kx, x) > 0$ because if $(Kx, x) = 0$ and $x \neq 0$, x and 0 will constitute *two* distinct solutions of the source problem with $F = 0$, thus violating the uniqueness property.

This completes the first part of the proof.

We now focus on showing the equivalence between (54,55) and the system (41,42), and the independence of the solution with respect to α.

Clearly, the solution d of the system (54,55) is also the solution of (56), since $\bar{K}d = PKPd = PF$ ($d = Pd \Leftrightarrow Q^Td = 0$). It is left to show that the vice versa also holds, i.e., solution d of (56) satisfies (54,55). We proceed by expressing the system (56) as a minimization problem where the functional Φ to be minimized is given by:

$$\Phi = \frac{1}{2}(PKPd, d) - (PF, d) + \frac{\alpha}{2}(Q^Td, Q^Td) \tag{58}$$

where $\alpha > 0$. $\bar{K}$ defined above is just the coefficient matrix of the linear system derived from Φ. Assume a decomposition $d = y + z$ where $y = Pd$. This implies the following relations:
$z = Q(Q^TQ)^{-1}Q^Td \Rightarrow (y, z) = 0$ or,
z is orthogonal to y and $Pz = 0$, $Py = y$.
Making use of these relations in the functional Φ, we can restate the minimization problem as follows:
Find a pair of orthogonal vectors (y, z) with $Py = y$, that minimizes

$$\Phi(y, z) = \frac{1}{2}(Ky, y) - (PF, y) + \frac{\alpha}{2}(Q^Tz, Q^Tz) \tag{59}$$

As can be easily observed, the solution pair (y, z) should satisfy:
$Q^Tz = 0$ and $Ky = PF$ or, equivalently (using the above relations),
$z = 0$ and $PKPy = PF$, $y = Py$ or, $PKPd = PF$, $d = Pd$, same as system (54,55), thus completing the equivalence proof.
The independence of the solution with respect to α follows directly from the expression for $\Phi(y, z)$.

Remark 1
For the case where K is strictly positive definite, another form of positive definite reformulation has been introduced in [25], yielding a symmetric positive definite system with respect to a non-Euclidian inner product.

3.2 Solution Methods for the Positive Definite System

The development of the positive definite coefficient matrix $\bar{K}$ makes the solution of the local system possible by a direct solver that does not require pivoting. Alternatively, it also provides the basis for the application of classical preconditioned iterative methods. $\bar{K}$ can be symbolically represented as:

$$\bar{K} = \begin{bmatrix} \bar{K}^L_{LL} & \bar{K}^L_{LB} & \bar{K}^L_{Ls} \\ \bar{K}^L_{BL} & \bar{K}^L_{BB} & \bar{K}^L_{Bs} \\ \bar{K}^L_{sL} & \bar{K}^L_{sB} & \bar{K}^L_{ss} \end{bmatrix} \tag{60}$$

where $\bar{K}^L_{LL} = K^L_{LL}$. The blocks in the matrix $\bar{K}$, except those associated with the interior degrees of freedom, do not necessarily have a banded structure and hence the direct solution might become expensive. A more practical approach would be to form an efficient preconditioner from $\bar{K}$ and apply it to one of the classical iterative methods for solving positive definite systems. One such preconditioner that has been used in our study is of block Gauss-Seidel type, given by:

$$\hat{K} = \begin{bmatrix} \bar{K}^L_{LL} & \bar{K}^L_{LB} & \bar{K}^L_{Ls} \\ 0 & \bar{K}^L_{BB} & \bar{K}^L_{Bs} \\ 0 & \bar{K}^L_{sB} & \bar{K}^L_{ss} \end{bmatrix} \tag{61}$$

To facilitate the description of solution algorithms, we introduce additional symbols and notations as described below:
The blocks in $\hat{K}$ and P that correspond to the interface degrees of freedom plus the local grid degrees of freedom at the boundary at the interface will be denoted by $\tilde{K}$ and $\tilde{P}$ respectively, i.e.,

$$\tilde{K} = \begin{bmatrix} \bar{K}^L_{BB} & \bar{K}^L_{Bs} \\ \bar{K}^L_{sB} & \bar{K}^L_{ss} \end{bmatrix}, \qquad \tilde{P} = \begin{bmatrix} P_{BB} & P_{Bs} \\ P_{sB} & P_{ss} \end{bmatrix}$$

Similarly, any vector with a "~" will include only interface degrees of freedom plus local grid degrees of freedom at the boundary at the interface. For e.g., the search direction v can be represented as

$$v = \begin{bmatrix} v^L_L & \tilde{v} \end{bmatrix}^T \equiv \begin{bmatrix} v^L_L & v^L_B & v_s \end{bmatrix}^T \tag{62}$$

We introduce an operator form $\varphi(\tilde{v})$ that represents the computational sequence which produces reactions $\tilde{f}$ (in the projected subspace) corresponding to the prescribed incremental displacement vector $\tilde{v}$. (This procedure ensures that $r^L_L = 0$ at every iteration). $\varphi(\tilde{v})$ constitutes the following steps:

$$r^L_L = -K^L_{LB} v^L_B, \qquad v^L_L = {K^L}^{-1}_{LL} r^L_L, \qquad f^{L\prime}_B = K^L_{BL} v^L_L + K^L_{BB} v^L_B, \qquad f'_s = 0, \qquad \tilde{f} = \tilde{P}\tilde{f}'.$$

The proposed PCG algorithm is indeed similar to the classical PCG procedure for positive definite systems. The following assertion clarifies this point further.
Assertion 3: If the initial guess for the solution d lies within the projected subspace, i.e., if $Q^T d = 0$ or equivalently, $Pd = d$, the search directions created by the application of the

preconditioner $\hat{K}$ will remain in the projected subspace.

Proof: We begin by evaluating the residual r corresponding to d:

$$r = PF - \bar{K}d = PF - PKPd \tag{63}$$

$$= P(F - Kd) \tag{64}$$

where the relations $Q^T d = 0$ and $Pd = d$ have been used. $r = [r_L^L \quad \tilde{r}]^T$ is in the projected subspace. Let us now apply the preconditioner $\tilde{K}$ to $\tilde{r}$ to obtain the search direction $\tilde{v}$:

$$\tilde{v} = \tilde{K}^{-1}\tilde{r} \tag{65}$$

We claim that $\tilde{P}\tilde{v} = \tilde{v}$, or, $\tilde{v}$ lies in the projected subspace. To prove this, consider the system:

$$\bar{K}q = f \tag{66}$$

where $f = [f_L^L \quad \tilde{f}]^T$ with $\tilde{f} = \tilde{r}$. Since $\tilde{P}\tilde{f} = \tilde{f}$, we have $Pf = f$ for any f_L^L. Let $f_L^L = \bar{K}_{LB}^L v_B^L + \bar{K}_{Ls}^L v_s$. It follows from the property of the positive definite operator $\bar{K}$ that the solution q of (66) satisfies $\tilde{P}\tilde{q} = \tilde{q}$. It is a simple matter to verify that q in (66) is given by $q = [0 \quad \tilde{v}]^T$.

Thus, we have $\tilde{P}\tilde{v} = \tilde{v}$, verifying the claim made above.

The resulting PCG algorithm for solving the local problem is summarized in Table 1. The left subscript is used to denote the local iteration count.

Table 1: The PCG Algorithm for Local Problem

Initialization

$${}_0\tilde{d} = {}^i\tilde{d}, \quad r_L^L = F_L^L - K_{LB}^L\, {}_0d_B^L, \quad {}_0d_L^L = K^{L^{-1}}_{LL} r_L^L,$$
$${}_0r_B^{L'} = F_B^L - K_{BL}^L\, {}_0d_L^L - K_{BB}^L\, {}_0d_B^L, \quad {}_0r_s' = 0, \quad {}_0\tilde{r} = \tilde{P}\ {}_0\tilde{r}'$$

$${}_0\tilde{b} = \tilde{K}^{-1}\ {}_0\tilde{r}$$
$${}_0\tilde{v} = {}_0\tilde{b}$$
$${}_0\tilde{f} = \varphi({}_0\tilde{v})$$

Do for $j = 1, 2...$until convergence

$${}_j\gamma = ({}_{j-1}\tilde{r}, {}_{j-1}\tilde{v})/({}_{j-1}\tilde{f}, {}_{j-1}\tilde{v})$$
$${}_j\tilde{d} = {}_{j-1}\tilde{d} + {}_j\gamma\ {}_{j-1}\tilde{v}$$
$${}_jd_L^L = {}_{j-1}d_L^L + {}_j\gamma\ {}_{j-1}v_L^L$$
$${}_j\tilde{r} = {}_{j-1}\tilde{r} - {}_j\gamma\ {}_{j-1}\tilde{f}$$
$${}_j\tilde{b} = \tilde{K}^{-1}\ {}_j\tilde{r}$$
$${}_j\beta = ({}_j\tilde{r}, {}_j\tilde{b})/({}_{j-1}\tilde{r}, {}_{j-1}\tilde{b})$$
$${}_j\tilde{v} = {}_j\tilde{b} + {}_j\beta\ {}_{j-1}\tilde{v}$$
$${}_j\tilde{f} = \varphi({}_j\tilde{v})$$

Remark 2

For ill-conditioned problems such as thin shells, some form of acceleration becomes necessary to speed up the convergence of the global-local iterative procedure. We adopt a two-parameter acceleration scheme to improve the rate of convergence of the hybrid composite grid scheme (HCG) presented in the previous sections. The two scalar acceleration parameters α and β are used to obtain the corrected displacements ${}^id^G$, ${}^id_s$ and ${}^id^L$ at the end of the current iteration i as follows:

$$ {}^id^G = {}^{i-1}d^G + \alpha v^G + \beta w^G \tag{67}$$
$$ {}^id_s = {}^{i-1}d_s + \alpha v_s + \beta w_s \tag{68}$$
$$ {}^id^L = {}^{i-1}d^L + \alpha v^L + \beta w^L \tag{69}$$

where w^G, w_s and w^L refer to the displacement increments in the previous global-local cycle on grids G^G, G_s and G^L respectively, and v^G, v_s and v^L stand for the "predicted" displacement increments in the three grids in the current cycle i. The parameters α and β

are obtained by minimizing the global energy functional Π while satisfying the constraints as explained below:

$$\Pi = \frac{1}{2}[(K^G({}^{i-1}d^G + \alpha v^G + \beta w^G), {}^{i-1}d^G + \alpha v^G + \beta w^G) \tag{70}$$

$$+(K^L({}^{i-1}d^L + \alpha v^L + \beta w^L), {}^{i-1}d^L + \alpha v^L + \beta w^L)] \tag{71}$$

$$-(F^G, {}^{i-1}d^G + \alpha v^G + \beta w^G) - (F^L, {}^{i-1}d^L + \alpha v^L + \beta w^L) \Rightarrow \overset{\min}{\alpha, \beta} \tag{72}$$

subject to:

$${}^i\phi^G \equiv \phi^G({}^{i-1}d^G + \alpha v^G + \beta w^G, {}^{i-1}d_s + \alpha v_s + \beta w_s) = 0 \tag{73}$$

and

$${}^i\phi^L \equiv \phi^L({}^{i-1}d^L + \alpha v^L + \beta w^L, {}^{i-1}d_s + \alpha v_s + \beta w_s) = 0 \tag{74}$$

Since the displacements at the end of the previous cycle (${}^{i-1}d^G$, ${}^{i-1}d^L$, ${}^{i-1}d_s$) and the displacement increments in the previous cycle (w^G, w^L, w_s) as well as the predicted increments in the current cycle (v^G, v^L, v_s) satisfy the constraints independently, the constraint equation will be satisfied for any set of values of α and β due to linearity and homogeneous nature of the equations (73) and (74). Hence the minimization can be carried out independent of the constraints. Minimization yields a system of two equations to be solved for α and β. Here we omit the details of implementation.

4 The Hybrid Domain Decomposition Technique

In this section, we present an alternative to the hybrid composite grid method, which is useful in cases where a global problem is not available to function as an auxiliary grid. To elaborate further, consider the situation where one only has the individual sub-domains or substructures and their corresponding grids (for example, grids G^G and G^L but no initial grid G^A), in addition to the interface grid. In the general case, one may have multiple substructures interconnected through a network of interface grids. The three-field hybrid variational form corresponding to this general case can be stated as:

$$\Pi = \sum_{k=1}^{N_{ss}}(\frac{1}{2}(d_k, K_k d_k) - (d_k, F_k)) + \sum_{i=1}^{N_I}\sum_{j=1}^{n_{ss}(i)}(\int_{S_{ij}} \lambda_{ij}(u_i - u_{ij})\, ds_{ij}) \Rightarrow \text{stationary} \tag{75}$$

where K_k and d_k denote respectively the stiffness matrix and displacement vector of substructure k, N_{ss} the number of substructures in the analysis, N_I the number of interfaces between the substructures, $n_{ss}(i)$ the number of substructures connected to the interface i; u_i is the interface element displacement field along the interface i, λ_{ij} the field of Lagrange multipliers for substructure j at interface i, and u_{ij} represents the displacement field for substructure j along interface i.

Following the usual discretization procedures that define interpolations for the displacements of the substructures and interface, as well as for the Lagrange multipliers, we arrive at the following system of equations:

$$Kd + Q\Lambda = F \tag{76}$$

$$Q^T d = 0 \tag{77}$$

The system (76,77) is indeed very similar to the "local" problem (41,42) within the hybrid composite grid iterative scheme presented earlier, except that unlike (41,42), (76) and (77) are defined not just on the local grids, but on the entire problem domain consisting of all the substructures and interfaces. In other words, Q^T, the assembled form of the constraint equations, now includes all the subdomain boundaries at any particular interface, and the block diagonal stiffness matrix in (76) is made up of diagonal blocks corresponding to stiffness matrices of all the subdomains or substructures in the problem, apart from, of course, the zero blocks corresponding to the interfaces. Accordingly, it is possible to develop single-level direct and iterative solution schemes for the source problem (76,77) by simply adopting the same principles presented for the direct and iterative solution of the "local" problem in the previous sections.

In the case of two substructures with a single interface, which corresponds to the example considered in the formulation of the hybrid composite grid method, matrices K and Q^T take the form:

$$K = \begin{bmatrix} K_{II} & K_{IB} & 0 \\ K_{BI} & K_{BB} & 0 \\ 0 & 0 & 0 \end{bmatrix} \quad Q^T = [0 \quad M^T \quad J^T] \tag{78}$$

where K_{II}, K_{IB} and K_{BB} are block-diagonal matrices given by:

$$K_{II} = \begin{bmatrix} K^G_{GG} & 0 \\ 0 & K^L_{LL} \end{bmatrix} \quad K_{IB} = \begin{bmatrix} K^G_{GB} & 0 \\ 0 & K^L_{LB} \end{bmatrix} \quad K_{BB} = \begin{bmatrix} K^G_{BB} & 0 \\ 0 & K^L_{BB} \end{bmatrix}$$

and matrices M^T and J^T have the structure:

$$M^T = \begin{bmatrix} M^{G^T}_B & 0 \\ 0 & M^{L^T}_B \end{bmatrix} \quad J^T = \begin{bmatrix} J^{G^T} \\ J^{L^T} \end{bmatrix} \tag{79}$$

We have grouped together degrees of freedom associated with all the substructure nodes except those at the boundary at the interface, with the subscript "$_I$", where as variables corresponding to all the substructure nodes at the boundary at the interface will be identified with the subscript "$_B$". This also obviates the need for grid identification, i.e., whether it is G^G or G^L.

The remaining steps in the solution of (76,77), namely development of the projection operator, formulation of the equivalent positive definite system and the subsequent direct or preconditioned iterative solution are analogous to those appearing in the procedure for the solution of the "local" problem presented earlier, with obvious modifications.

4.1 A Two-level Hybrid Domain Decomposition Method

Even though a natural auxiliary grid is absent in the hybrid domain decomposition technique, one may be constructed to be used in a two-level iterative solution scheme. The proposed auxiliary grid corresponds to the so-called collocation problem, in which the subdomain boundaries meeting at the interface are constrained to deform according to the prescribed, displacement interpolation of the interface. In the auxiliary problem, the finite element displacement field for the subdomain boundary at the interface is interpolated using the same interpolants as for the interface elements. In other words,

$$u_B = N_s d_s \tag{80}$$

which yields

$$d_B = N_s(X_B) d_s \equiv T^B_s d_s \tag{81}$$

where X_B are the coordinates of the substructure boundary nodes at the interface. T^B_s is a prolongation operator relating the interface element degrees of freedom to the finite element

degrees of freedom in the substructure at the boundary at the interface. The resulting auxiliary problem can be deduced as follows:
Given the current solution ${}^i d$, the auxiliary correction v_0 should minimize

$$\frac{1}{2}(K({}^i d + T_0^1 v_0), {}^i d + T_0^1 v_0) - ({}^i d + T_0^1 v_0, F) \tag{82}$$

where T_0^1 is the prolongation operator consisting of T_s^B and the identity operators corresponding to the interface degrees of freedom themselves and the substructure interior degrees of freedom:

$$T_0^1 \equiv \begin{bmatrix} I & 0 \\ 0 & T_s^B \\ 0 & I \end{bmatrix} \tag{83}$$

The minimization yields the auxiliary problem:

$$K_0 v_0 = {}^i r_0 \tag{84}$$

where

$$K_0 = {T_0^1}^T K T_0^1, \qquad {}^i r_0 = {T_0^1}^T {}^i r, \qquad {}^i r = F - K\, {}^i d \tag{85}$$

The proposed two-level hybrid domain decomposition method consists of smoothing of equivalent positive definite system to capture the oscillatory part of the solution as previously described, and the direct solution of the collocation-based auxiliary grid problem to resolve the smooth components of the error. We omit the implementational details, for the sake of conciseness.

5 Performance Study

In this section we present select numerical examples to demonstrate the performance of the hybrid composite grid method (HCG), and compare its performance to the single-level and two-level hybrid domain decomposition techniques (HDD), both described in the previous sections. Specifically, numerical results are presented for a representative 2-dimensional problem, namely that of an L-shaped domain; and for two shell problems, one that of a stiffened panel with a hole under in-plane and pressure loading, and the other a cylindrical

shell. The first two problems can be classified as a global-local problem, while the third one is not a typical global-local problem due to the relatively large size of the "local" problem chosen.

CPU times for the hybrid composite grid method are given for the case when the local problem is solved directly using the equivalent, positive definite operator as well as when several relaxation sweeps are applied using preconditioned conjugate gradient method up to a relative error tolerance of 10^{-1} to 10^{-3} in the Euclidian norm of the residual in the local region. For problems where the formation of the positive definite operator $\bar{K}$ may be expensive, smoothing procedure of the local problem only to a prescribed relative tolerance offers an attractive alternative. The CPU estimates presented later for both approaches substantiate this point. Of course, in either case, the major part of the solution procedure for the local problem (formation and factorization of the positive definite operator for direct solution, or formation and factorization of the diagonal blocks in the preconditioner for iterative solution) is pre-computed, before the start of the hybrid composite grid solution procedure. As mentioned earlier, the auxiliary grid stiffness matrix is also available in the factorized form at the start of the solution procedure.

For the purpose of comparison, the problems were also formulated in accordance with the hybrid domain decomposition (HDD) method corresponding to the three-field hybrid formulation, which were then solved by means of the direct solver and also the single- and the two-level iterative solvers applied to the transformed, positive definite system.

5.1 The L-shaped Domain Problem

Figure 3 shows the initial mesh as well as the local or finer mesh around the re-entrant corner, that is independent of the initial mesh. Both meshes were modeled using 4 node, bi-linear quadrilateral elements. The independent interface between the meshes was discretized using 2 node, linear elements. The Lagrange multipliers were taken to be constants for the boundary elements of the grids G^G and G^L at the interface, to ensure stability [23]. The initial grid, which is also the auxiliary grid, consists of 2296 nodes whereas the local grid has 736 nodes. The interface grid carries a total of 79 nodes.

Table 2 summarizes the results for the L-shaped domain problem. The advantage of the iterative solution over the direct solver for the local problem is evident from the CPU times

presented for the HCG method. Also apparent is the superiority of the hybrid composite grid iterative method with the iterative local solver over the domain decomposition approach for this particular problem. The excellent convergence rate of the composite grid iterative method is illustrated by the relatively small number of iterations to achieve the prescribed tolerance of 10^{-8}. Among the hybrid domain decomposition (HDD) techniques, the single-level iterative solver was found to be the most efficient in terms of CPU time. The explanation for this lies in the fact that the other two choices, namely the direct solver and the two-level iterative solver, involve expensive computations — the formation and factorization of the equivalent positive definite operator $\bar{K}$ in the former case and the positive definite operator K_0 for the collocation problem in the latter. It is possible to make all the three methods more efficient by employing sparse direct solvers [27], as opposed to the standard skyline solvers, but the major beneficiaries will be the direct solver and the two-level iterative solver. Of course, such improvements in the efficiency can also be made to the solution of the local problem within the hybrid composite grid (HCG) method.

We would like to mention that for this 2-dimensional example, the pre-conditioner was applied only to the interior degrees of freedom in all cases of iterative solution where preconditioner is applicable. In other words, $\tilde{K}$ within the preconditioner $\hat{K}$ was replaced by the identity matrix. This simplification doesn't affect the performance of the iterative methods significantly for well-conditioned problems.

5.2 The Stiffened Panel Problem

In this case, as shown in Figure 4, the problem is that of a rectangular panel with two stiffeners and with a central circular hole. The panel is subjected to uniform in-plane loading as well as uniform pressure loading, resulting in bending. Only one symmetric half of the domain is analyzed. Both the panel and stiffener were discretized using 3-node, flat shell triangular elements, [26], with 6 degrees of freedom per node. The initial grid has a total of 823 nodes. The refined local mesh around the circular hole has a total of 201 nodes. The independent interface discretization carries a total of 33 nodes. The interface is made up of 2-node elements with linear interpolation for all the six degrees of freedom. The Lagrange multipliers were taken to be piece-wise constants, as before.

As in the L-shaped domain problem, the optimum performance is achieved with the

iterative solver for the local problem, as can be verified from the results presented in Table 3. Also, the hybrid composite grid method outperforms the corresponding hybrid domain decomposition approach for this problem by approximately 40% in terms of the CPU time. Within the HDD approach, the single-level preconditioned conjugate gradient method once again has the lowest CPU time.

5.3 The Cylindrical Shell Problem

The final example problem corresponds to that of a cylindrical shell (Figure 5) fixed at one end and carrying point loads at the other end resulting in cantilever-type loading. As in the previous example, the shell was modeled with 3-node, flat shell elements. The uniform initial discretization resulted in a total of 780 nodes. The "local" region was taken to be one half of the cylindrical shell starting from the fixed end, the discretization of which carries a total of 600 nodes. The curved, circumferential interface between the grids G^G and G^L was modeled with 2-node elements as in the case of the panel example, and carried a total of 30 nodes. As mentioned in the introduction, this problem is not a typical global-local problem because of the relatively large size of the local problem.

The fact that the convergence of the composite grid iterative scheme is not impaired significantly by a larger local region can be verified from the results presented in Table 4, where results are given for thick ($\frac{r}{t} = 20$) as well as thin ($\frac{r}{t} = 200$) shells (here r is the radius and t is the thickness of the shell). It may be noted that for a thin shell, the direct solution of the local problem seems to be a better choice, compared to the iterative solution, while for the thick shell the iterative solver outperforms the direct solver as in the previous two examples. As may be expected, in this example, the iterative hybrid domain decomposition approach, especially the single-level preconditioned conjugate gradient method, performs better than the various versions of the hybrid composite grid method.

Acknowledgment

The authors gratefully acknowledge the support of NASA Langley under research grant No. NAG-1-1356, and that of the National Science Foundation NYI award ECS-9257203.

References

[1] C.D. Mote, 'Global-local finite element', Int. J. Numer. Meth. Eng., Vol. 3, pp. 565-574, (1971).

[2] A.K. Noor, 'Global-local methodologies and their application to nonlinear analysis', Finite elements in Analysis and Design, Vol. 2, pp.333-346, (1986).

[3] J.Fish and S.Markolefas, 'Adaptive global-local refinement strategy based on the interior error estimates of the h-method', Int. J. Numer. Meth. Eng., Vol. 37, pp.827-838, (1994).

[4] I.Babuska, S.Strouboulis, C.S.Upadhyay and S.K.Gangaraj, 'A posteriori estimation and adaptive control of the pollution-error in the h-version of the finite element method', Technical Note BN-1175, institute for Physical Science and Technology, University of Maryland, College Park, MD.

[5] S.F. McCormick and J.W.Thomas, 'The fast adaptive composite grid (FAC) method for elliptic equations', Mathematics of Computation, Vol. 46, pp. 439-456, (1986).

[6] J. Bramble, R.E. Ewing, J.E. Pasciak and A.H. Schatz, 'A preconditioning technique for the efficient solution of problems with local grid refinement', Comp. Meth. Appl. Mech. Eng., Vol. 67, pp. 149-159 (1988).

[7] J.E.Flaherty, P.K.Moore and C.Ozturan, 'Adaptive overlapping methods for parabolic systems', in Adaptive Methods for Partial Differential Equations (Edited by J.E. Flaherty, P.J. Paslow, M.S. Shephard and J.D. Vasilakis), SIAM (1989).

[8] J.D. Whitcomb, 'Iterative global-local finite element analysis', Computers and Structures, Vol. 40, No. 4, pp. 1027-1031, (1991).

[9] J. Fish and V. Belsky, 'Multi-grid method for periodic heterogeneous media. Part 2: Multiscale modeling and quality control in multidimensional case', accepted in Comp. Meth. Appl. Mech. Eng., (1994).

[10] A. Brandt, 'Multi-level adaptive solutions to boundary-value problems', Mathematics of Computations, Vol. 31, pp. 333-390, (1977)

[11] J.Fish, 'The s-version of the finite element method', SCOREC report,18-1990, Rensselaer Polytechnic Institute, Troy, NY, (1990).

[12] J. Fish, S.Markolefas, R.Guttal, P.Nayak, 'On adaptive multilevel superposition of finite element meshes for linear elastostatics', Applied Numerical Mathematics, Vol. 14, pp. 135-164, (1994).

[13] T. Belytschko, J.Fish, and A.Bayliss, 'The spectral overlay on finite elements for problems with high gradients', Comp. Meth. Appl. Mech. Eng., Vol. 81, pp. 71-89 (1990).

[14] H.Yserentant, 'On the multilevel splitting of finite element spaces', Numer. Math. pp. 379-412, (1986).

[15] J.N.Reddy and D.H. Robbins, 'Theories and computational models for composite laminates', Appl. Mech. Rev., Vol. 47, No.1, pp. 147-169, (1994).

[16] A.K.Noor, W.S.Burton and J.M. Peters, 'Predictor-Corrector Procedures for Stress and free Vibration Analyses of Multilayered Composite Plates and Shells', Comp. Meth. Appl. Mech. Eng., Vol. 82, pp. 341-363 (1990).

[17] N.F.Knight, J.B.Ransom, O.H.Griffin, and D.M. Thompson, 'Global/Local Methods Research Using a Common Structural Analysis Framework', Finite Element Analysis and Design, Vol. 9, pp. 91-112, (1991).

[18] K.M.Mao and C.T.Sun, 'A refined Globa-Local Finite Element Analysis Method', Int. J. Numer. Meth. Eng., Vol. 32, pp. 29-43, (1991).

[19] J.B. Ransom, S.L.McCleary and M.A. Aminpour, 'A new interface element for connecting independently modeled substructures', 33rd AIAA/ASME/ASCE/AHS/ASC SDM Conference, Dallas, TX, pp. 109-119, (1992)

[20] J.Fish, V. Belsky and M.Pandheeradi, 'Iterative and Direct Solvers for Interface Problems with Lagrange Multipliers', Proceedings of the Third National Symposium on Large-Scale Structural Analysis for High-Performance Computers and Workstations, Norfolk, VA, (1994). Also to appear in Computing Systems in Engineering.

[21] C.Farhat and F.X. Roux, 'An unconventional domain decomposition method for an efficient parallel solution of large scale finite element systems,' SIAM J. Sci. Stat. Comput., Vol. 13, pp. 379-396, (1992).

[22] C. Farhat, 'A Lagrange Multiplier based divide and conquer finite element algorithm', Computing Systems in Engineering, Vol. 2, No. 2/3, pp. 149-156, (1991).

[23] C. Bernardi, Y. Maday and A. Patera, 'A new nonconforming approach to domain decomposition: the mortar element method', in: H.Brezis and J.L. Lions, eds., Nonlinear Partial Differential Equations and their Applications, Pitman, London, (1989).

[24] P.E. Gill and W.Murray, Numerical Methods for Constraint Optimization, academic Press, London, (1974).

[25] J.H. Bramble and J.E. Pasciak, 'A Preconditioned Technique for Indefinite Systems resulting from Mixed approximations of Elliptic Problems', Math. Comput., Vol. 50, No. 181, pp. 1-17, (1988).

[26] J. Fish and T. Belytschko, 'Stabilized rapidly convergent 18-degrees-of-freedom flat shell triangular element', Int.j.numer.methods eng., Vol. 33, pp. 149-162, (1992).

[27] A. George and J.W.H. Liu, 'The evolution of the minimum degree ordering algorithm', CS-87-06, North York, Ontario York University, (1987).

List of Tables

List of Figures

Table 2: Hybrid Composite Grid Iterative Solution of the L-shaped Domain Problem

Formulation	Local solution method for HCG/Solution method for HDD	# of iter	CPU sec.
HCG	Direct	10	58
HCG	PCG	10	28
HDD	Direct		149
HDD	PCG (single-level)	89	39
HDD	two-level	9	61

Table 3: Hybrid Composite Grid Iterative Solution of the Panel Problem

Formulation	Local solution method for HCG/Solution method for HDD	# of iter	CPU sec.
HCG	Direct	25	110
HCG	PCG	25	101
HDD	Direct		265
HDD	PCG (single-level)	105	138
HDD	two-level	8	169

Table 4: Hybrid Composite Grid Iterative Solution of the Cylindrical Shell Problem

$\frac{\text{radius}}{\text{thickness}}$	Formulation	Local solution method for HCG/Solution method for HDD	# of iter	CPU sec.
20	HCG	Direct	30	229
	HCG	PCG	39	148
	HDD	Direct		307
	HDD	PCG (single-level)	78	120
	HDD	two-level	7	171
200	HCG	Direct	41	250
	HCG	PCG	74	251
	HDD	Direct		307
	HDD	PCG (single-level)	93	126
	HDD	two-level	22	200

Patch Test for Interfaces

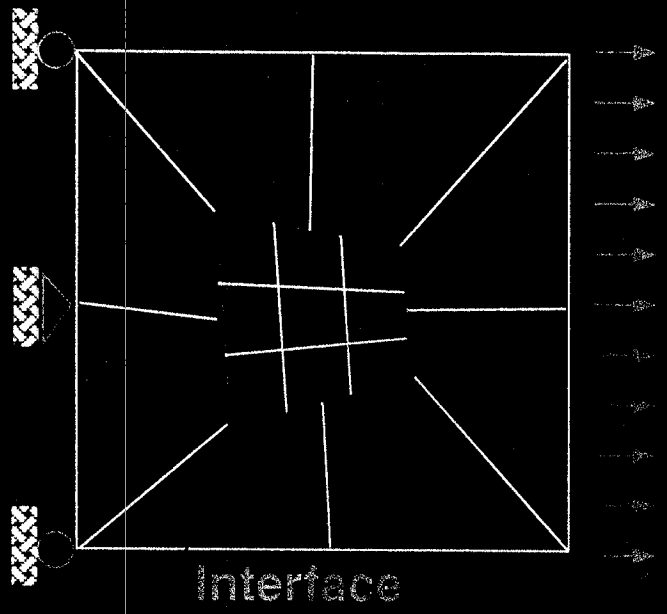

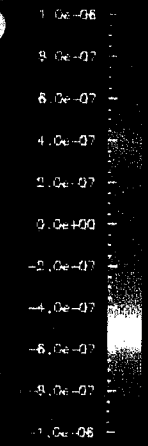

Hybrid Formulation

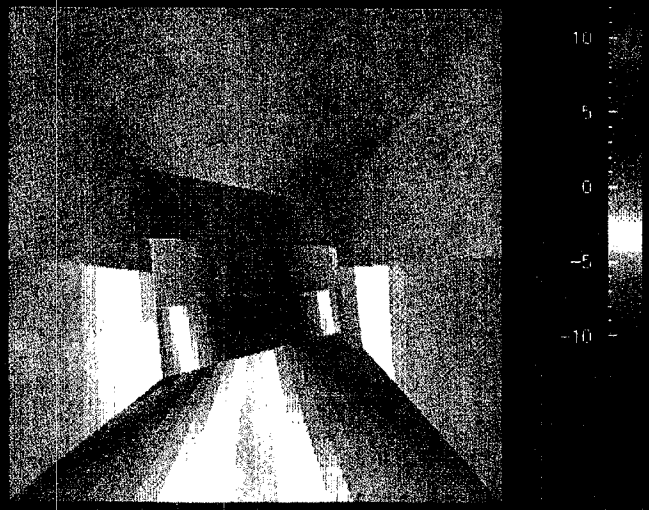

Collocation (8 linear elements)

Collocation (4 cubic elements)

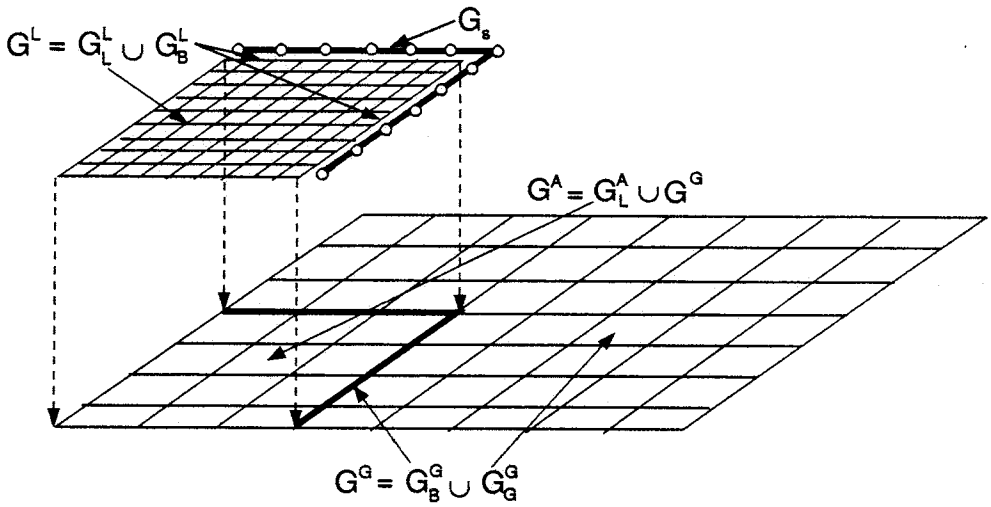

Figure 2

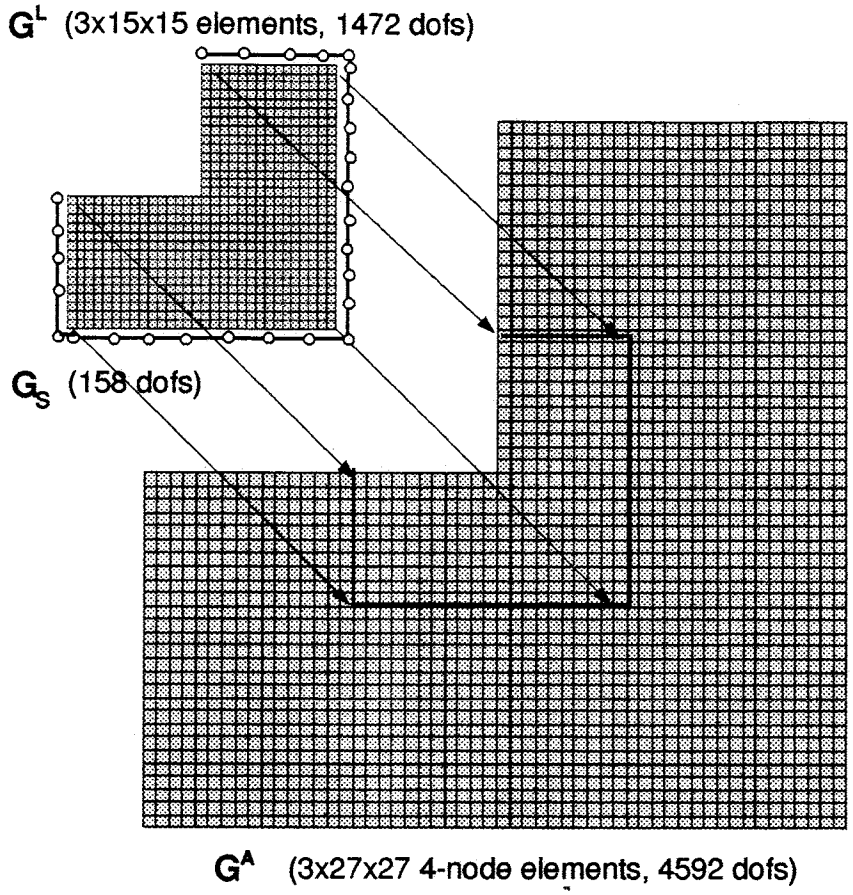
G^L (3x15x15 elements, 1472 dofs)
G_S (158 dofs)
G^A (3x27x27 4-node elements, 4592 dofs)

Figure 3

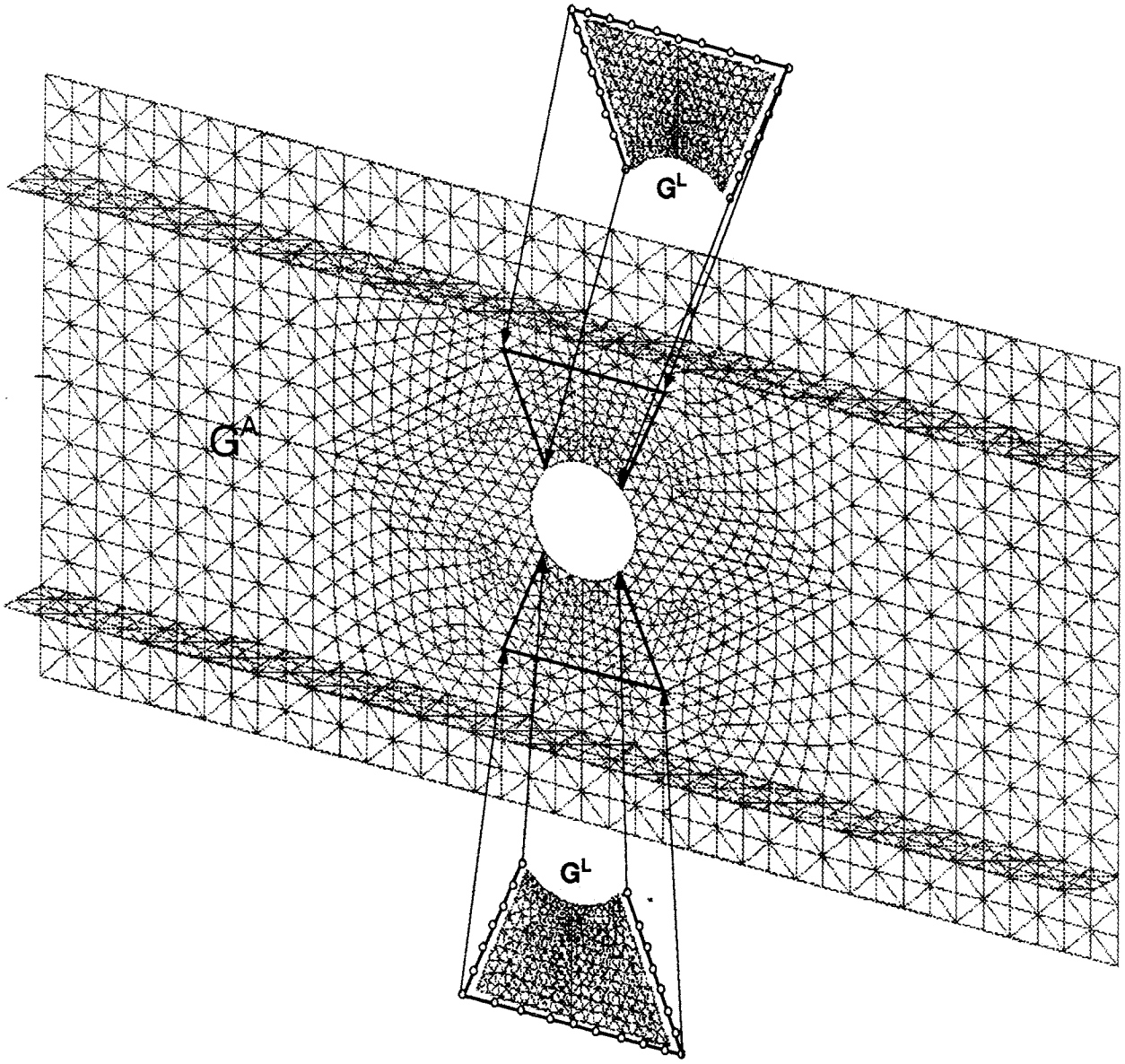

Figure 4

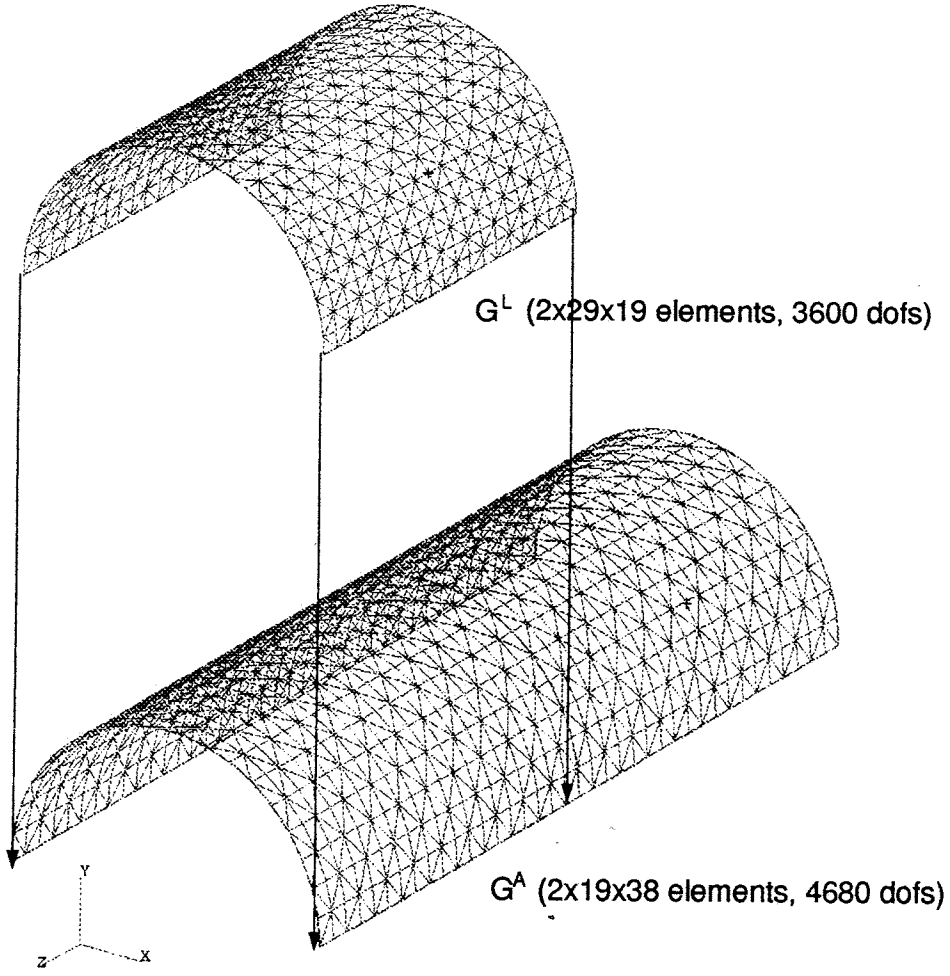
G^L (2x29x19 elements, 3600 dofs)
G^A (2x19x38 elements, 4680 dofs)
Y
Z
X

Figure 5